Langmuir
Article
pubs.acs.org/Langmuir

Thermodynamic Characterization of Acacia Gum−β-Lactoglobulin Complex Coacervation

Leïla Aberkane,[†] Jordane Jasniewski,*[,†] Claire Gaiani,[†] Joël Scher,[†] and Christian Sanchez[‡]

[†]*Laboratoire d'Ingénierie des Biomolécules, Nancy Université, INPL-ENSAIA, 2 Avenue de la Forêt-de-Haye, F-54505 Vandoeuvre-lès-Nancy cedex 5, France, and* [‡]*2UMR 1208 IATE, UM2-INRA-SupAgro-CIRAD, 2 place Viala, 34060 Montpellier cedex 1v, France*

Received February 17, 2010. Revised Manuscript Received June 15, 2010

The interactions of β-lactoglobulin (BLG) with total acacia gum (TAG) in aqueous solutions have been investigated at pH 4.2 and 25 °C. Isothermal titration calorimetry (ITC) has been used to determine the type and magnitude of the energies involved in the complexation process of TAG to BLG. Dynamic light scattering (DLS), electrophoretic mobility (μ_E), turbidity measurements (τ), and optical microscopy were used as complementary methods on the titration mode to better understand the sum of complicated phenomena at the origin of thermodynamic behavior. Two different binding steps were detected. Thermodynamic parameters indicate a first exothermic step with an association constant K_{a1} of $(48.4 \pm 3.6) \times 10^7$ M^{-1} that appeared to be mostly enthalpy-driven. A positive heat capacity change was obtained corresponding at the signature for electrostatic interactions. The second binding step, 45 times less affinity ($K_{a2} = (1.1 \pm 0.1) \times 10^7$ M^{-1}), was largely endothermic and more entropy-driven with a negative value of heat capacity change, indicative of a hydrophobic contribution to the binding process. The population distribution of the different species in solution and their sizes were determined through DLS. Dispersion turbidity of particles markedly increased and reached a maximum at a 0.015 TAG/BLG molar ratio. Largely more numerous coacervates appeared at this molar ratio (0.015) and two different kinds of morphologies were noticed for the large coacervates. Above the TAG/BLG molar ratio of 0.015, dispersions turbidity decreased, which might be due to an excess of negative charges onto particles as revealed by electrophoretic mobility measurements. The results presented in this study should provide information about the thermodynamic mechanisms of TAG/BLG binding processes and will facilitate the application of the formed supramolecular assemblies as functional ingredients in food and nonfood systems.

Introduction

Complex coacervation between oppositely charged proteins and polysaccharides, and more generally between oppositely charged macromolecules, is an ubiquitous colloidal phenomenon involved in the structuring of many biological systems.[1,2] Oppositely charged proteins and polysaccharides interact mainly through electrostatic interactions, which induce the formation of various supramolecular entities such as complexes, aggregated complexes, and coacervates. The structure and solubility of these supramolecular entities depend on a number of parameters, especially structure, flexibility, and charge density of biopolymers, quality of solvent, ionic strength, protein to polysaccharide molar ratio, and total biopolymer concentration.[2−11] Interestingly, original functional properties of these different entities can be used both in food and nonfood applications.[1,2,12]

Since its discovery in 1911,[13] the interest in complex coacervation has been fluctuating. However, owing to the biological significance of protein−polysaccharide electrostatic interactions and the huge industrial potential of protein−polysaccharide complexes and coacervates, including the advent of nanobiotechnologies and design of biomimetic systems, studies on complex coacervation have exponentially grown during the past decade.[2] In recent years major scientific advances, mainly dealing with protein−polymer systems, concerned phase-ordering

*Corresponding author. E-mail: jordane.jasniewski@ensaia.inpl-nancy.fr.

(1) Schmitt, C.; Aberkane, L.; Sanchez, C. Protein-polysaccharide complexes and coacervates. In *Handbook of Hydrocolloids*; Phillips, G. O., Williams, P. A., Eds.; Glyndwr University: Wrexham, U.K., 2009; pp 421−476.

(2) Turgeon, S. L.; Schmitt, C.; Sanchez, C. *Curr. Opin. Colloid Interface Sci.* **2007**, *12*(4−5), 166–178.

(3) Bungenburg de Jong, H. G. Crystallisation-coacervation-floculation. In *Colloid Science*; Kruyt, H. G., Ed.; Elsevier: Amsterdam, 1949; pp 232−258.

(4) Burgess, D. J. Complex coacervation: Microcapsule formation. In *Macromolecular complexes in chemistry and Biology*; Dubin, P. L., Bock, J., Davis, R., Schulz, D. N., Thies, C., Eds.; Springer Verlag: Berlin, 1994; pp 281−300.

(5) Schmitt, C.; Sanchez, C.; Désobry-Banon, S.; Hardy, J. Structure and technofunctional properties of protein-polysaccharide complexes: A review. *Crit. Rev. Food Sci. Nutrition* **1998**, *38*, (8), 689−753.

(6) Doublier, J. L.; Garnier, C.; Renard, D.; Sanchez, C. Protein-polysaccharide interactions. *Curr. Opin. Colloid Interface Sci.* **2000**, *5*, (3−4), 202−214.

(7) de Kruif, C. G.; Tuinier, R. Polysaccharide protein interactions. *Food Hydrocolloids* **2001**, *15*, (4−6), 555−563.

(8) Turgeon, S. L.; Beaulieu, M.; Schmitt, C.; Sanchez, C. Protein-polysaccharide interactions: phase-ordering kinetics, thermodynamic and structural aspects. *Curr. Opin. Colloid Interface Sci.* **2003**, *8*, (4−5), 401−414.

(9) de Kruif, C. G.; Weinbreck, F.; de Vries, R. Complex coacervation of proteins and anionic polysaccharides. *Curr. Opin. Colloid Interface Sci.* **2004**, *9*, (5), 340−349.

(10) Cooper, C. L.; Dubin, P. L.; Kayitmazer, A. B.; Turksen, S. Polyelectrolyte-protein complexes. *Curr. Opin. Colloid Interface Sci.* **2005**, *10*, (1−2), 52−78.

(11) McClements, D. J. Non-covalent interactions between proteins and polysaccharides. *Biotechnol. Adv.* **2006**, *24*, (6), 621−625.

(12) Dickinson, E. Colloid science of mixed ingredients. *Soft Matter* **2006**, *2*, (8), 642−652.

(13) Tiebackx, F. W. Gleichzeitige Ausflockung zweier Kolloide. *Z. Chem. Ind. Kolloide* **1911**, *8*, (4), 198−201.

(14) Sanchez, C.; Renard, D.; Robert, P.; Schmitt, C.; Lefebvre, J. Structure and rheological properties of acacia gum dispersions. *Food Hydrocolloids* **2002**, *16*, (3), 257−267.

(15) Sanchez, C.; Mekhloufi, G.; Renard, D. Complex coacervation between β-lactoglobulin and Acacia gum: A nucleation and growth mechanism. *J. Colloid Interface Sci.* **2006**, *299*, (2), 867−873.

(16) Leisner, D.; Imae, T. Interpolyelectrolyte complex and coacervate formation of poly(glutamic acid) with a dendrimer studied by light scattering and SAXS. *J. Phys. Chem. B* **2003**, *107*, (32), 8078−8087.

dynamics during complex coacervation[14,15] and the structure at different scales of coacervates.[16−24]

Despite these significant progresses, understanding the multiple facets of complexation between proteins and polysaccharides remains an experimental and theoretical challenge. Among the most important issues is a better understanding of thermodynamic mechanisms at the origin of binding processes and stabilization of macromolecular assemblies. It is well-known that the driving force leading to the formation of protein−polysaccharide complexes is the decrease of the total electrostatic free energy of the mixture.[25,26] The overall decrease in free energy results predominantly from a favorable enthalpic contribution arising from the electrostatic and possibly non-Coulombic interactions between biopolymers, and a favorable entropic contribution arising from the release of counterions[9,26] and water molecules[27] upon biopolymer interactions. These favorable contributions are counterbalanced by an unfavorable loss of configurational entropy of macromolecules[28] and ordering of water at the complex interface[27] and an unfavorable enthalpy due to the desolvation of polar groups.[29] Nevertheless, the large gain of entropy due to the release of counterions is thought to be the main driving force in the formation of protein−polysaccharide complexes. This assumption is supported by the suppression of complex formation above a critical ionic strength. In this case, the entropic gain arising from the release of counterions disappears because counterions concentration becomes more or less equivalent in the solvent phase and in the neighborhood of biopolymers.[3,30−32] It should be noted that the release of counterions was experimentally demonstrated in the lysozyme/polystyrene sulfonate system using a deuterated tetramethylammonium counterion.[33]

Now, while endothermic signals were effectively recorded by calorimetry on a number of systems involving proteins and strong polyelectrolytes (e.g., refs 34 and 35), indicating that complexation was driven by a gain in entropy, exothermic signals were recorded on all protein−polysaccharide systems studied in the literature,[36−42] indicating that complexation was driven by enthalpy. Such an apparent contradiction motivated our interest in studying in some details of the thermodynamic properties of interacting oppositely charged proteins and polysaccharides. The β-lactoglobulin (BLG)/total acacia gum (TAG)/water system was used as a model. This model has been characterized in detail by us and others in the past,[14,15,17,32,43−47] but never from a thermodynamic point of view. Thermodynamic binding parameters between BLG and TAG were determined using isothermal titration calorimetry (ITC). In parallel using the same titration approach, to better understand thermodynamic results, the structure at different scales and surface charges of complexes were probed, using dynamic light scattering (DLS), electrophoretic mobility (μ_E), turbidity measurements (τ), and optical microscopy.

Materials and Methods

Materials. BLG powder (lot JE 003-6-922) was provided by Davisco Foods International, Inc. (Lesueur, MN). The powder composition was (g/100 g) 93.6% protein ($N \times 6.38$), 4.6%

(17) Weinbreck, F.; Rollema, H. S.; Tromp, R. H.; deKruif, C. G. Diffusivity of Whey Protein and Gum Arabic in Their Coacervates. *Langmuir* **2004**, *20*, (15), 6389−6395.
(18) Cousin, F.; Gummel, J.; Ung, D.; Boué, F. Polyelectrolyte-protein complexes: Structure and conformation of each specie revealed by SANS. *Langmuir* **2005**, *21*, (21), 9675−9688.
(19) Gummel, J.; Boué, F.; Demé, B.; Cousin, F. Charge stoichiometry inside polyelectrolyte-protein complexes: A direct SANS measurement for the PSSNa-lysozyme system. *J. Phys. Chem. B* **2006**, *110*, (49), 24837−24846.
(20) Kayitmazer, A. B.; Bohidar, H. B.; Mattison, K. W.; Bose, A.; Sarkar, J.; Hashidzume, A.; Russo, P. S.; Jaeger, W.; Dubin, P. L. Mesophase separation and probe dynamics in protein-polyelectrolyte coacervates. *Soft Matter* **2007**, *3*, (8), 1064−1076.
(21) Kayitmazer, A. B.; Strand, S. P.; Tribet, C.; Jaeger, W.; Dubin, P. L. Effect of polyelectrolyte structure on protein - Polyelectrolyte coacervates: Coacervates of bovine serum albumin with poly(diallyldimethylammonium chloride) versus chitosan. *Biomacromolecules* **2007**, *8*, (11), 3568−3577.
(22) Wang, X.; Li, Y.; Wang, Y. W.; Lal, J.; Huang, Q. Microstructure of β-lactoglobulin/pectin coacervates studied by small-angle neutron scattering. *J. Phys. Chem. B* **2007**, *111*, (3), 515−520.
(23) Chodankar, S.; Aswal, V. K.; Kohlbrecher, J.; Vavrin, R.; Wagh, A. G. Structural study of coacervation in protein-polyelectrolyte complexes. *Phys. Rev. E* **2008**, *78*, (3).
(24) Schmidt, I.; Cousin, F.; Huchon, C.; Boué, F.; Axelos, M. A. V. Spatial structure and composition of polysaccharide-protein complexes from small angle neutron scattering. *Biomacromolecules* **2009**, *10*, (6), 1346−1357.
(25) Tolstoguzov, V. B. Food Proteins and Their Application. In *Food Proteins and Their Applications*; Damodaran, S., Paraf, A., Eds.; Marcel Dekker, Inc.: New York, 1997; pp 171−198.
(26) de Vries, R.; Cohen Stuart, M. Theory and simulations of macroion complexation. *Curr. Opin. Colloid Interface Sci.* **2006**, *11*, (5), 295−301.
(27) Jelesarov, I.; Bosshard, H. R. Isothermal titration calorimetry and differential scanning calorimetry as complementary tools to investigate the energetics of biomolecular recognition. *J. Mol. Recognit.* **1999**, *12*, (1), 3−18.
(28) Leavitt, S.; Freire, E. Direct measurement of protein binding energetics by isothermal titration calorimetry. *Curr. Opin. Struct. Biol.* **2001**, *11*, (5), 560−566.
(29) Freire, E. In *Thermodynamic in Drug Design. High Affinity and Selectivity*; Proceedings of The Chemical Theatre of Biological Systems, Bozen, Italy, 2004; Beilstein-Institut: Bozen, Italy, 2004; pp 1−13.
(30) Burgess, D. J.; Carless, J. E. Manufacture of gelatin/gelatin coacervate microcapsules. *Int. J. Pharm.* **1985**, *27*, (1), 61−70.
(31) Seyrek, E.; Dubin, P. L.; Tribet, C.; Gamble, E. A. Ionic Strength Dependence of Protein-Polyelectrolyte Interactions. *Biomacromolecules* **2003**, *4*, (2), 273−282.
(32) Weinbreck, F.; de Vries, R.; Schrooyen, P.; de Kruif, C. G. Complex Coacervation of Whey Proteins and Gum Arabic. *Biomacromolecules* **2003**, *4*, (2), 293−303.
(33) Gummel, J.; Cousin, F.; Boué, F. Counterions release from electrostatic complexes of polyelectrolytes and proteins of opposite charge: A direct measurement. *J. Am. Chem. Soc.* **2007**, *129*, (18), 5806−5807.
(34) Ball, V.; Winterhalter, M.; Schwinte, P.; Lavalle, P.; Voegel, J. C.; Schaaf, P. Complexation mechanism of bovine serum albumin and poly(allylamine hydrochloride). *J. Phys. Chem. B* **2002**, *106*, (9), 2357−2364.
(35) Feng, X.; Pelton, R.; Leduc, M.; Champ, S. Colloidal complexes from poly(vinyl amine) and carboxymethyl cellulose mixtures. *Langmuir* **2007**, *23*, (6), 2970−2976.
(36) Girard, M.; Turgeon, S. L.; Gauthier, S. F. Thermodynamic Parameters of β-Lactoglobulin-Pectin Complexes Assessed by Isothermal Titration Calorimetry. *J. Agric. Food Chem.* **2003**, *51*, (15), 4450−4455.
(37) Ziegler, A.; Seelig, J. Interaction of the Protein Transduction Domain of HIV-1 TAT with Heparan Sulfate: Binding Mechanism and Thermodynamic Parameters. *Biophys. J.* **2004**, *86*, (1), 254−263.
(38) Gonçalves, E.; Kitas, E.; Seelig, J. Binding of oligoarginine to membrane lipids and heparan sulfate: Structural and thermodynamic characterization of a cell-penetrating peptide. *Biochemistry* **2005**, *44*, (7), 2692−2702.
(39) Harnsilawat, T.; Pongsawatmanit, R.; McClements, D. J. Characterization of β-lactoglobulin-sodium alginate interactions in aqueous solutions: A calorimetry, light scattering, electrophoretic mobility and solubility study. *Food Hydrocolloids* **2006**, *20*, (5), 577−585.
(40) Schmitt, C.; Palma Da Silva, T.; Rami-Shojaei, C. B. S.; Frossard, P.; Kolodziejczyk, E.; Leser, M. E. Effect of time on the interfacial and foaming properties of β-lactoglobulin/acacia gum electrostatic complexes and coacervates at pH 4.2. *Langmuir* **2005**, *21*, (17), 7786−7795.
(41) Zhu, J.; Zhang, X.; Li, D.; Jin, J. Probing the binding of flavonoids to catalase by molecular spectroscopy. *J. Mol. Struct.* **2007**, *843*, (1−3), 38−44.
(42) Chung, K.; Kim, J.; Cho, B. K.; Ko, B. J.; Hwang, B. Y.; Kim, B. G. How does dextran sulfate prevent heat induced aggregation of protein?: The mechanism and its limitation as aggregation inhibitor. *Biochim. Biophys. Acta* **2007**, *1774*, (2), 249−257.
(43) Mekhloufi, G.; Sanchez, C.; Renard, D.; Guillemin, S.; Hardy, J. pH-Induced Structural Transitions during Complexation and Coacervation of β-Lactoglobulin and Acacia Gum. *Langmuir* **2005**, *21*, (1), 386−394.
(44) Schmitt, C.; Sanchez, C.; Despond, S.; Renard, D.; Thomas, F.; Hardy, J. Effect of protein aggregates on the complex coacervation between β-lactoglobulin and acacia gum at pH 4.2. *Food Hydrocolloids* **2000**, *14*, (4), 403−413.
(45) Schmitt, C.; Sanchez, C.; Lamprecht, A.; Renard, D.; Lehr, C.-M.; de Kruif, C. G.; Hardy, J. Study of β-lactoglobulin/acacia gum complex coacervation by diffusing-wave spectroscopy and confocal scanning laser microscopy. *Colloids Surf., B* **2001**, *20*, (3), 267−280.
(46) Schmitt, C.; Sanchez, C.; Thomas, F.; Hardy, J. Complex coacervation between β-lactoglobulin and acacia gum in aqueous medium. *Food Hydrocolloids* **1999**, *13*, (6), 483−496.
(47) Weinbreck, F.; Nieuwenhuijse, H.; Robijn, G. W.; de Kruif, C. G. Complexation of Whey Proteins with Carrageenan. *J. Agric. Food Chem.* **2004**, *52*, (11), 3550−3555.

moisture, and 1.8% ash. The mineral composition was (g/100 g) 0.002 Mg^{2+}, 0.025 Ca^{2+}, 0.900 Na^{+}, 0.007 K^{+}, and 0.050 Cl^{-}. Powdered TAG (lot no. 97 J 716) was a gift from CNI Company (Rouen, France). The powder composition was (g/100 g) 89.4% polysaccharide, 0.6% protein, 7.0% moisture, and 3.0% ash. The mineral composition was (g/100 g) 0.200 Mg^{2+}, 0.610 Ca^{2+}, 0.032 Na^{+}, and 0.900 K^{+}.

Sodium hydroxide and hydrochloric acid were of analytical grade.

Methods. *Preparation of β-Lactoglobulin (BLG) and Total Acacia Gum (TAG) Stock Dispersions.* To eliminate excess salts, BLG and TAG were extensively dialyzed (Spectra/Por, MWCO: 6−8000) against ultra pure deionized water and freeze-dried. Stock dispersions of BLG and TAG at 0.6 and 1.8 wt % total biopolymer concentration, respectively, were prepared by gradually adding the freeze-dried biopolymer to ultra pure deionized water (18.2 mΩ resistivity) under gentle stirring at 20 ± 1 °C for at least 2 h. The pH of BLG dispersion was adjusted to 4.7 (pH corresponding to the lowest BLG solubility) with HCl (1N). Dispersions were stored at 4 °C for about 18 h to allow for complete hydration of macromolecules. Then, stock dispersions were centrifuged for 40 min at 10 000 rpm to remove insoluble material and air bubbles. Dispersions were filtered through a 0.22 μm syringe filter (Millipore, Bedford, USA).

The concentration of BLG dispersions was checked by UV−visible spectroscopy (Ultrospec 4000 UV−visible, Pharmacia Biotech, England) using specific extinction coefficient of 9.6 dl/cm·g at 278 nm, as determined experimentally. The optical density at 278 nm was corrected for turbidity. The final pH was adjusted to 4.2 (the maximum of interaction in BLG/TAG system as determined by Sanchez et al., 2006).

Isothermal Titration Calorimetry (ITC). An isothermal titration calorimeter (VP-ITC, Microcal Inc., Northampton, MA) was used to determine the enthalpic and entropic changes resulting from the titration of BLG (0.6 wt %) by TAG dispersion (1.8 wt %) at 25, 35, 45, and 50 °C. The dispersions were degassed under vacuum for 5 min. A portion of 10 μL of TAG dispersion was injected sequentially into a 1.428 mL titration cell initially containing BLG dispersion. Each injection lasted 20 s, and there was an interval of 150 s between successive injections. The temperature of dispersions in the titration cell was 25 °C. A rotating 250 μL Hamilton microsyringe ensuring constant stirring of the whole mixed dispersion at a speed of 260 rpm ensured the homogenization during injection. The heat of dilution from the blank titration of ultra pure deionized water into BLG dispersion and TAG dispersion into ultra pure deionized water were measured, and the dilution heats were subtracted from the raw data. For TAG, the heat of dilution was in the range of −1.0 ∼ −0.2 μcal, and for BLG solution, the heat of dilution was about −0.02 μcal. Data acquisition and analyses were performed using Microcal Origin software (v.7.0). The "Two Sets of Sites" binding model, provided with software, was used to fit binding isotherms. Thermodynamic parameters, including the binding constant (K_a), enthalpy changes (ΔH_m), and binding stoichiometry (N) (molar ratio BLG:TAG), were calculated by iterative curve fitting of the binding isotherms. For site 1 and site 2, there are:

$$K_{a1} = \frac{\Theta_1}{(1-\Theta_1)[X]} \qquad K_{a2} = \frac{\Theta_1}{(1-\Theta_2)[X]} \tag{1}$$

$$X_t = [X] + M_t(n_1\Theta_1 + n_2\Theta_2) \tag{2}$$

K_a = binding constant; N = binding stoichiometry; M_t and $[M]$ are bulk and free concentration of macromolecule in V_o; V_o = titration cell volume; X_t and $[X]$ are bulk and free concentration of ligand (Acacia gum); Θ = fraction of sites occupied by ligand X.

Solving eq 1 for Θ_1 and Θ_2 and then substituting into eq 2 gives:

$$X_t = [X] + \frac{N_1 M_t [X] K_{a1}}{1 + [X] K_{a1}} + \frac{N_2 M_t [X] K_{a2}}{1 + [X] K_{a2}} \tag{3}$$

Clearing eq 3 of fractions and collecting like terms leads to a cubic equation of the form:

$$[X]^3 + pX^2 + q[X] + r = 0 \tag{4}$$

where

$$p = \frac{1}{K_{a1}} + \frac{1}{K_{a2}} + (N_1 + N_2)M_t - X_t$$

$$q = \left(\frac{N_1}{K_{a2}} + \frac{N_2}{K_{a1}}\right)M_t - \left(\frac{1}{K_{a1}} + \frac{1}{K_{a2}}\right)X_t + \frac{1}{K_{a1}K_{a2}}$$

$$r = \frac{-X_t}{K_{a1}K_{a2}} \tag{5}$$

Equations 4 and 5 can be solved for [X] either in closed form or (as done in Origin) numerically by using Newton's method if parameters N_1, N_2, K_{a1}, and K_{a2} are assigned. Both Θ_1 and Θ_2 may then be obtained from eq 1 above.

The heat content after any injection is equal to:

$$Q = M_t V_0 (N_1\Theta_1\Delta H_{m1} + N_2\Theta_2\Delta H_{m2}) \tag{6}$$

After a similar correction for displaced volume, the pertinent calculated heat effect for the i injection is:

$$\Delta Q(i) = Q(i) + \frac{dV_i}{V_0}\left[\frac{Q(i) + Q(i-1)}{2}\right] - Q(i-1) \tag{7}$$

which may be used in the Marquardt algorithm to obtain best values for the fitting parameters (ΔH_m, K_a, and N).

The variation of Gibbs free energy of mixing was calculated using the well-known relationship $\Delta G_m = -RT \ln K_a$.[48]

Entropy changes were then calculated using $\Delta G_m = \Delta H_m - T\Delta S_m$.

From the binding enthalpy ΔH_m measured at temperatures (T) ranging from 298 to 323 K, the heat capacity change (ΔC_p) was calculated using the relationship $\Delta C_p = d(\Delta H_m)/dT$.

Measurements were carried out in triplicate.

Dynamic Light Scattering (DLS) and Electrophoretic Mobility Measurements. DLS and electrophoretic mobility measurements upon injection of TAG dispersion into BLG dispersion were performed at 25 °C and pH 4.2 using a Nanosizer ZS equipment (HPPS 5001, Malvern Instrument, England). Measurements were done under the same experimental conditions as in ITC experiments except that samples were diluted 10 times before measurement to avoid detector saturation.

The apparatus is equipped with a 4 mW He/Ne laser emitting at 633 nm, a measurement cell, a photomultiplier, and a correlator. The samples for size measurements were placed in vertical cylindrical cuvettes (10 mm diameter). Scattering intensity was measured at a scattering angle of 173° relative to the source using

(48) Pierce, M. M.; Raman, C. S.; Nall, B. T. Isothermal Titration Calorimetry of Protein-Protein Interactions. *Methods* **1999**, *19*, (2), 213−221.

an avalanche of photodiode detector. This setup allows considerable reduction of the signal due to multiple scattering events and enables working in slightly turbid media. Intensity autocorrelation functions were analyzed by the CONTIN algorithm to determine the distribution of translational z-averaged diffusion coefficient of particles, D_T ($m^2 \cdot s^{-1}$). The D_T parameter is related to the hydrodynamic radius (R_h) of particles through the Stokes−Einstein relationship $D_T = k_B T/6\pi\eta R_h$ where η is the solvent viscosity (Pa·s), k_B is the Boltzmann constant (1.38×10^{-23} $N \cdot m \cdot k^{-1}$), T is the absolute temperature (K), and R_h (m) is the equivalent hydrodynamic radius of a sphere having the same diffusion coefficient than the particles.[49]

Results from the CONTIN algorithm allow the determination of both R_h distribution and respective amplitude of each particle population. In the following, the hydrodynamic diameter D_h ($2 \times R_h$) is displayed.

Electrophoretic mobility measurements (μ_E) were performed by means of laser Doppler electrophoresis. The sample was put in a standard capillary electrophoresis cell equipped with gold electrodes. The electrophoretic mobility from the blank titration of ultra pure deionized water into BLG dispersion and TAG dispersion into ultra pure deionized water were measured as control. For the purposes of clarity, electrophoretic mobility units ($\mu m \cdot cm \cdot s^{-1} \cdot V^{-1}$) will be referred to emu in the following. Each measurement was performed in triplicate.

Turbidity Measurement and Optical Microscopy. The evolution of turbidity was followed during titration of BLG dispersion by TAG dispersion in the spectrophotometer cell, under exactly the same experimental conditions as in ITC experiments at 25 °C and pH 4.2. A spectrophotometer (Ultrospec 4000 UV/Visible, Pharmacia Biotech, England) was used at a wavelength of 633 nm. Samples were placed in a 10 mm path length cuvette, and then turbidity were calculated as $\tau = (-1/L) \ln(I_0/I_t)$, with L as the optical path length (cm), I_t as the transmitted light intensity, and I_0 as the incident light intensity.

An epi-fluorescence microscope (Leica DMRB, Wetzlar, Germany) was used to monitor the TAG/BLG molar ratio-induced structural changes upon titration of BLG (1.5 wt %) dispersion by TAG (4.5 wt %) dispersion. A 10 μL sample was taken from mixed dispersions and put between glass slides. Pictures were recorded using a charge-coupled device (CCD) camera through an image processor (Kappa ImageBase 2.5) at × 40 magnification. The contrast and the brightness of pictures were processed by the ImageJ freeware (version 1.40) to better visualize light fluctuations.

Results

Thermodynamic Characterization of Interactions between TAG and BLG. ITC was used to probe enthalpy changes associated with interactions between oppositely charged TAG and BLG. The heat flow versus time profile and the corresponding binding isotherm resulting from injections of aliquots of TAG dispersion into BLG dispersion at pH 4.2 and 25 °C are shown in Figure 1. The peak areas correspond to the energy released or absorbed by the cell containing BLG after each TAG injection. A sequence of strong successive exothermic peaks of decreasing intensity was initially observed (Figure 1A). As the titration proceeded, the (released) binding energy progressively decreased and then reversed to endothermic after 10 injections (0.015 TAG/BLG molar ratio). The last sequence of weaker endothermic peaks tended to a state of thermodynamic stability toward the end of injections, while remaining slightly negative. At 25 °C and pH 4.2, binding isotherms between TAG and BLG were then characterized by an exothermic−endothermic sequence with the heat of dilution in the range of −6.0 to 0.5 μcal.

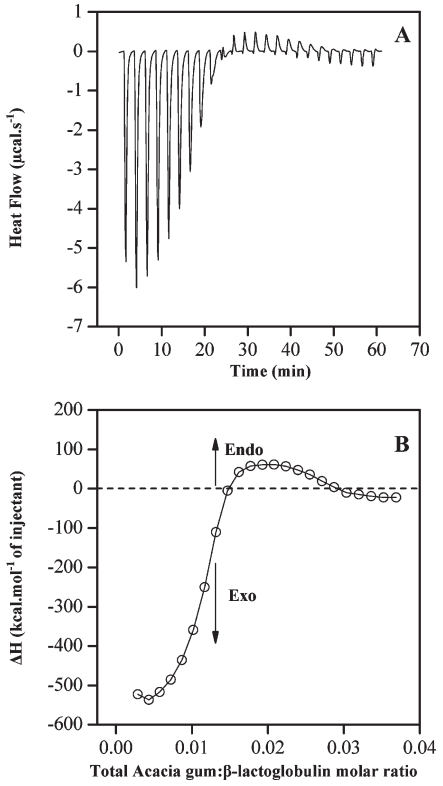

Figure 1. (A) Thermogram and (B) binding isotherm corresponding to the titration of an aqueous dispersion of TAG (1.8 wt %) into an aqueous dispersion of BLG (0.6 wt %) at pH 4.2 and 25 °C. The experiments were made in triplicate.

To better understand thermodynamic changes during titration, binding isotherms were fitted using different binding models provided by the Microcal Origin software. Best-fit results were obtained using the "Two Sets of Sites" binding model (minimization of χ^2). However, the existence of two different and independent binding sites has no clear physical foundations when dealing with interactions between two macromolecules. Indeed, because of the nonspecific nature of interactions and particularly the carboxyl group as the only interacting group on the TAG, the exothermic−endothermic sequence is more likely indicative of two different steps involved in the BLG−TAG complexation rather than two different binding sites. For that reason, the expression "2-sites model" was replaced here with the more appropriate "2-stages structuring model". Rather, the binding model better indicated the presence of two distinct structuring stages during interaction between TAG and BLG. It is interesting to note that the "Two Sets of Sites" was also applied for the interactions between BLG and pectins, but results were discussed exclusively in terms of a two-stage structuring model.[36] The binding stoichiometry (N) of TAG/BLG complexes, binding constant (K_a), enthalpy (ΔH_m), and entropy (ΔS_m) changes and variation of Gibbs free energy (ΔG_m) found for these two stages are indicated in Table 1 (first stage) and Table 2 (second stage). During the first structuring stage (Table 1), TAG and BLG interacted with a high affinity (K_{a1}: $(48.4 \pm 3.6) \times 10^7$ M^{-1}), and binding was predominantly enthalpically driven with a very strong ΔH_{m1} of (-578.7 ± 7.6) kcal·mol^{-1}. However, unfavorable entropic contributions were in the same range

(49) Tanford, C. *Physical Chemistry of Macromolecules*; John Wiley and Sons: New York, 1961.

Table 1. Thermodynamic Parameters of First Stage of Binding between BLG and TAG Obtained from the Titration of an Aqueous Dispersion of TAG (1.8 wt %) into an Aqueous Dispersion of BLG (0.6 wt %) at pH 4.2 and Various Temperatures

temperature (K)	$N \times 10^4$	K_a (M^{-1}) $\times 10^7$	ΔH_m (kcal·mol^{-1})	$T\Delta S_m$ (kcal·mol^{-1})	ΔG_m (kcal·mol^{-1})
298.15	110.5 ± 0.2	48.4 ± 3.6	−578.7 ± 7.6	−566.4 ± 8.4	−12.2 ± 0.7
308.15	41.5 ± 0.2	19.0 ± 3.6	−90.8 ± 12.8	−79.2 ± 13.0	−11.6 ± 0.2
318.15	65.0 ± 0.2	244.5 ± 15.9	157.4 ± 3.3	171.0 ± 2.9	−13.5 ± 0.4
323.15	75.0 ± 0.0	852.0 ± 43.5	107.4 ± 9.4	122.3 ± 8.9	−14.8 ± 0.5

Table 2. Thermodynamic Parameters of Second Stage of Binding between BLG and TAG Obtained from the Titration of an Aqueous Dispersion of TAG (1.8 wt %) into an Aqueous Dispersion of BLG (0.6 wt %) at pH 4.2 and Various Temperatures

temperature (K)	$N \times 10^4$	K_a (M^{-1}) $\times 10^7$	ΔH_m (kcal·mol^{-1})	$T\Delta S_m$ (kcal·mol^{-1})	ΔG_{mi} (kcal·mol^{-1})
298.15	127.0 ± 0.1	1.1 ± 0.1	145.8 ± 8.9	158.5 ± 4.3	−12.7 ± 4.5
308.15	121.5 ± 0.3	0.6 ± 0.0	63.3 ± 4.7	71.3 ± 2.4	−8.0 ± 2.3
318.15	90.0 ± 0.1	6.9 ± 0.4	−44.3 ± 0.8	−33.3 ± 0.5	−11.0 ± 0.2
323.15	78.0 ± 0.4	19.0 ± 1.4	−48.4 ± 2.6	−37.4 ± 1.5	−11.0 ± 1.1

($T\Delta S_{m1}$: (−566.4 ± 8.4) kcal·mol^{-1}), indicating that an equilibrium between enthalpic and entropic contributions prevailed. From the TAG/BLG stoichiometry ($N_1 = (110.5 \pm 0.2) \times 10^{-4}$), we found that about 90 BLG dimers interacted with TAG during the first stage. On the other hand, the second structuring stage (Table 2) was characterized by a favorable binding entropy ($T\Delta S_{m1}$: (158.5 ± 4.3) kcal·mol^{-1}) and an unfavorable enthalpy (ΔH_{m1}: (145.8 ± 8.9) kcal·mol^{-1}). About 80 BLG dimers were involved in the interaction process with TAG ($N_2 = (127.0 \pm 0.1) \times 10^{-4}$), but with a lower affinity than during the first stage (K_{a1}: $(1.1 \pm 0.1) \times 10^7$ M^{-1}). The changes in Gibbs free energy was negative and not significantly different (∼12−13 kcal·mol^{-1}) for the two structuring stages (Tables 1 and 2).

The effect of temperature was investigated in the temperature range from 25 to 50 °C. The first objective was to check whether other weak energy interactions (hydrophobic interactions and hydrogen bonding) played a significant role in complexation between BLG and TAG. The second objective was to calculate the heat capacity changes ΔC_p, which are highly sensitive to the interactions between macromolecule residues and solvent molecules.[27,50,51] In particular, the heat capacity of binding has been shown to be extremely useful in predicting the surface-exposed polar and nonpolar surface area change upon ligand binding onto macromolecules.[52,53]

Two structuring stages were observed during titration of BLG by TAG for all temperatures applied (Figure 2). However, the prevalence of enthalpic or entropic contributions during the two stages was highly dependent on the temperature. At 25 and 35 °C, an exothermic−endothermic sequence was recorded during titration, indicating that the first structuring stage was driven by enthalpy, whereas the second one was driven by entropy (Tables 1 and 2). At 45 and 50 °C, the heat flow versus time profile revealed that during titration heat was initially absorbed then released (Figure 2A). Binding isotherms then displayed an endothermic−exothermic sequence (Figure 2B). Binding enthalpy was positive and unfavorable during the first structuring stage, whereas it was negative and favorable during the second one (Tables 1 and 2). On the other hand, binding entropy was favorable (positive) during the first structuring stage, whereas it was unfavorable (negative) during the second one. A last minor while interesting point concerns the binding enthalpy recorded at the end of the different titrations. As observed at 25 °C, final binding enthalpies were negative at all temperatures considered and became even increasingly negative reaching the end of the experiment.

The temperature dependence of the binding enthalpy ΔH_m determined during the two structuring stages of BLG/TAG mixtures is shown in Figure 3. The slope of the relationship of ΔH_m versus T describes the molar heat capacity change, ΔC_p, for the BLG−TAG interaction. The ΔC_p was 28.5 kcal·mol^{-1}·K^{-1} for the first stage and −8.3 kcal·mol^{-1}·K^{-1} for the second stage, with linear correlation coefficients of 0.88 and 0.97, respectively. The fit was obviously worse for the first stage, but there was no doubt that ΔC_p was large and positive. In the temperature range considered, ΔC_p was not temperature-dependent. The different signs of the ΔC_p clearly indicated different mechanisms of interaction between macromolecules or complexed macromolecules and solvent. In addition, with increasing temperature, the strength of interaction between BLG and TAG decreased during the first structuring stage and increased during the second one.

It was also observed that, despite the large variations in the measured binding enthalpies or calculated binding entropies, the Gibbs free energy ΔG_m was almost insensitive to the temperature (Tables 1 and 2). The relationship between the binding enthalpies ΔH_m and entropies $T\Delta S_m$ was then drawn as determined for the two structuring stages (Figure 4). As expected an almost perfect linear relationship was obtained, indicating that any change in enthalpy is accompanied by a similar change in entropy, that is, an entropy−enthalpy compensation occurred.

Structural Characterization of TAG/BLG Mixtures. To better understand the complex shape of binding isotherms, the structure of mixed dispersions upon titration of BLG by TAG was characterized, following the same experimental procedure that was used for ITC. Experiments were performed at 25 °C, the temperature usually selected to study thermodynamic properties of protein/polysaccharide mixtures by ITC.

Hydrodynamic Diameter (D_h) of TAG/BLG Complexes. The hydrodynamic diameter (D_h) of BLG and TAG was determined at pH 4.2 and 25 °C before the titration experiment (results not shown). The BLG dispersion was characterized by a single monodispersed peak with a hydrodynamic diameter of 4.8 nm. A similar value has been reported previously.[40,44,54] It accounted

(50) Ladbury, J. E.; Williams, M. A. The extended interface: measuring non-local effects in biomolecular interactions. *Curr. Opin. Struct. Biol.* **2004**, *14*, (5), 562−569.

(51) Olsson, T. S. G.; Williams, M. A.; Pitt, W. R.; Ladbury, J. E. The Thermodynamics of Protein-Ligand Interaction and Solvation: Insights for Ligand Design. *J. Mol. Biol.* **2008**, *384*, (4), 1002−1017.

(52) Spolar, R. S.; Ha, J. H.; Record, M. T., Jr. Hydrophobic effect in protein folding and other noncovalent processes involving proteins. *Proc. Natl. Acad. Sci. U.S.A.* **1989**, *86*, (21), 8382−8385.

(53) Baker, B. M.; Murphy, K. P. Dissecting the energetics of a protein-protein interaction: the binding of ovomucoid third domain to elastase. *J. Mol. Biol.* **1997**, *268*, (2), 557−569.

(54) Renard, D. *Etude de l'agrégation et de la gélification des protéines globulaires: application à la betalactoglobuline*; Nante University: Nante, France, 1994.

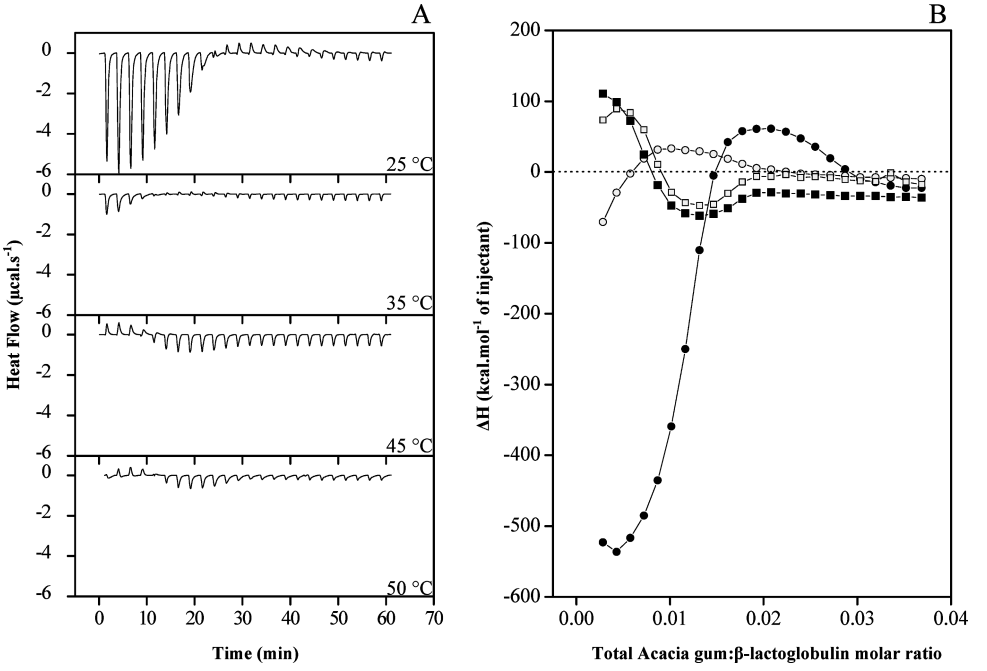

Figure 2. (A) Thermograms corresponding to the titration of an aqueous dispersion of TAG (1.8 wt %) into an aqueous dispersion of BLG (0.6 wt %) at pH 4.2 and different temperatures. (B) Binding isotherm corresponding to the various titration experiments. ●, 25 °C; ○, 35 °C; ■, 45 °C and □, 50 °C.

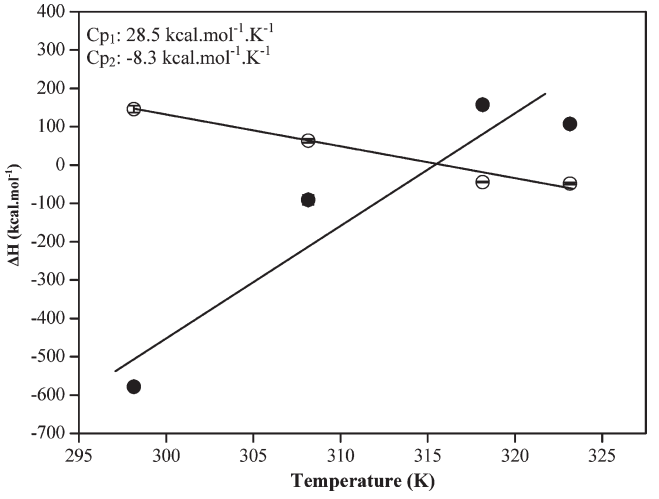

Figure 3. Temperature dependence of ΔH_{m1} (●) and ΔH_{m2} (○) for the binding of TAG (1.8 wt %) to BLG (0.6 wt %) at pH 4.2 and 25 °C.

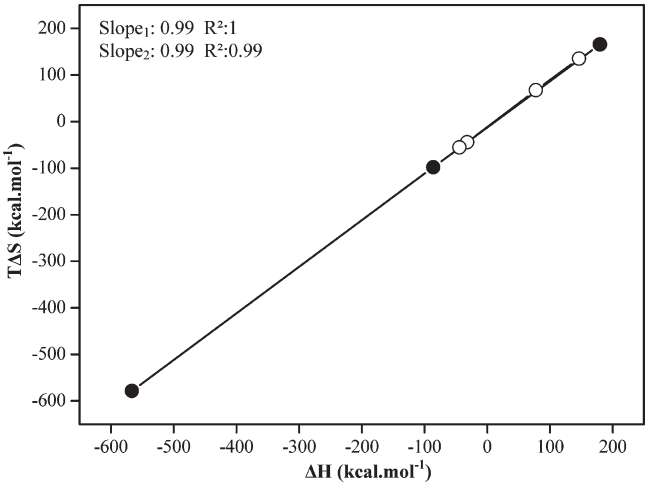

Figure 4. Enthalpy−entropy compensation plot for the TAG−BLG binding reaction at the first (●) and second step (○) of binding at pH 4.2 and 25 °C.

for equilibrium between monomeric and dimeric forms of the protein. The TAG sample revealed the presence of polydisperse macromolecules. This is mainly due to the complex nature of the gum that is composed of various molecular fractions.[55] While polydispersity implies considering DLS results with great care, the average hydrodynamic diameter measured was around 30−40 nm, which compares reasonably with values previously reported.[55]

The D_h of particles obtained during titration of BLG by TAG is shown in Figure 5. The first remark is that upon injection of the first TAG aliquote, that is, at a TAG/BLG molar ratio of 0.001, the D_h of complexes was ~850 nm. This diameter did not change after the second injection but considerably increased after the third one, reaching values above 2000 nm (Figure 5). The D_h values obtained with the third and the fifth injection were hardly reliable, which explains the dashed rectangle drawn in Figure 5. However, results indicated major structuring events in this range of TAG/BLG molar ratios. Above this range, the D_h decreased down to a minimal value of ~250 nm, reached after about 9−10 injections. The D_h of complexes remained steady until the 16th injection (TAG/BLG molar ratio: 0.024) and then increased up to another steady value of 300−340 nm (see inset of Figure 5) until the end of the titration experiment. It is further important to note that a second minor population of particles (10−30% of the total intensity) appeared after the fourth injection, with D_h above 5000 nm (results not shown). The D_h of these particles decreased upon further titration of BLG by TAG until approximatively the 16th injection, and then the second population of particles disappeared.

(55) Renard, D.; Lavenant-Gourgeon, L.; Ralet, M. C.; Sanchez, C. Acacia senegal Gum: Continuum of Molecular Species Differing by Their Protein to Sugar Ratio, Molecular Weight, and Charges. *Biomacromolecules* **2006**, *7*, (9), 2637−2649.

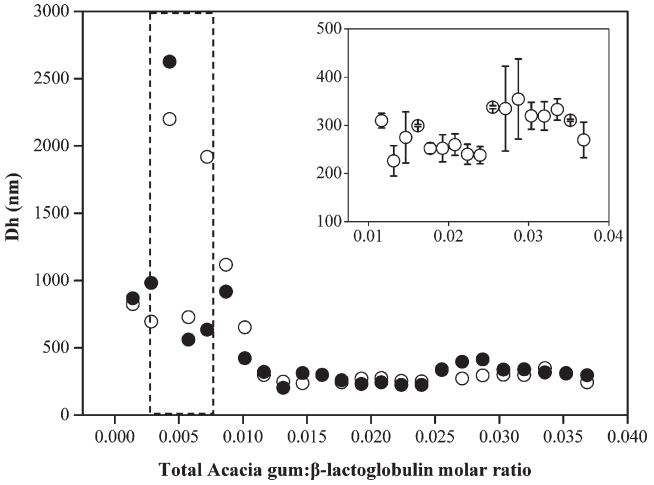

Figure 5. Evolution of the diameter of particles as a function of the TAG/BLG molar ratio during the titration of an aqueous dispersion of TAG (0.18 wt %) into an aqueous dispersion of BLG (0.06 wt %) at pH 4.2 and 25 °C. ● and ○ represent two independent experiments.

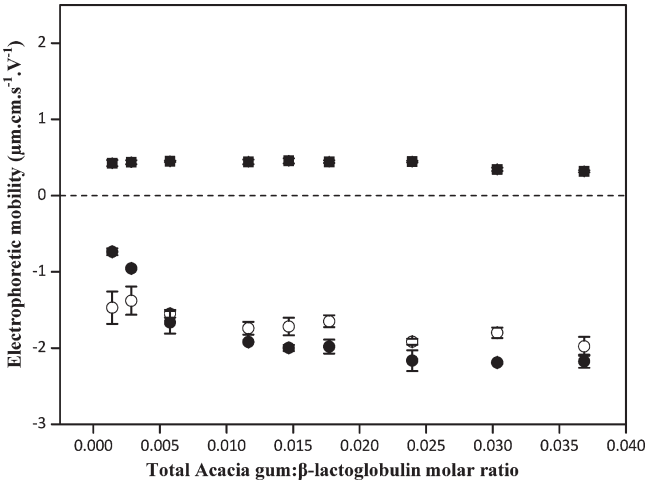

Figure 6. Evolution of electrophoretic mobility ($\mu m \cdot cm \cdot s^{-1} \cdot V^{-1}$) as a function of the TAG/BLG molar ratio during the titration of an aqueous dispersion of TAG (0.18 wt %) into an aqueous dispersion of BLG (0.06 wt %): ●, water into an aqueous dispersion of BLG (0.6 wt %); ■, an aqueous dispersion of TAG (1.8 wt %); ○, into water at pH 4.2 and 25 °C. The experiments were made in triplicate.

Electrophoretic Mobility of TAG/BLG Complexes. As complex formation between proteins and polysaccharides is mainly controlled by electrostatic interactions, electrophoretic mobility (μ_E) measurements were used to extract information on total surface charges of BLG, TAG, and complexed TAG/BLG as function of the TAG/BLG molar ratio (Figure 6). The measurements were determined at pH 4.2 and 25 °C.

The absolute values of electrophoretic mobility were found to be lower for BLG than for TAG. The BLG μ_E was positive and relatively stable ((0.320 ± 0.015) to (0.420 ± 0.018) $\mu m \cdot cm \cdot s^{-1} \cdot V^{-1}$) during titration by ultra pure deionized water. The variation of the BLG μ_E depended on the charge balance between the amino and the carboxylic groups carried by the protein. The electrophoretic mobility from the blank titration of TAG dispersion into ultra pure deionized water was negative in the pH considered (pH 4.2), due to the presence of glucoronic acid residues in the gum ($pK_a < 3.6$), and slightly increased (from (-1.47 ± 0.21) to (-1.97 ± 0.12) $\mu m \cdot cm \cdot s^{-1} \cdot V^{-1}$) with increasing TAG concentration.

The μ_E values of mixed dispersion obtained during titration of BLG by TAG were also negative and are shown in Figure 6. The electrophoretic mobility increased until the 8th injection of TAG aliquot (TAG/BLG molar ratio: 0.012). Starting from this point, the mixed μ_E displayed a similar whole evolution than TAG alone, indicating a good accessibility of the polysaccharide to the solvent. This highlighted the main contribution of TAG to the μ_E evolution of a mixed dispersion. The μ_E remained steady until the 12th injection (TAG/BLG molar ratio: 0.017) and then increased up to another steady value until the end of experiment.

The marked effect of this experiment was the control of μ_E value by BLG at low TAG/BLG molar ratio and by TAG at high TAG/BLG molar ratio. These results were in agreement with those found by Schmitt and co-workers (2000).[44]

Microstructural Evolution of TAG/BLG Complexes. Turbidity measurements (τ) were made according to the titration procedure of ITC experiments to give more information about the binding transition points. TAG dispersion is added incrementally to a highly dilute BLG dispersion, and the turbidity (τ) due to complex formation was measured (Figure 7).

The turbidity measurement showed a more complex dependence on TAG/BLG molar ratio. The first addition of TAG aliquot induced a slight increase of turbidity. This turbidity remained constant and increased after the fourth injection (TAG/BLG molar ratio: 0.005) until reaching a maximum after about 8−9 injections. These results suggest an increase in the amount of insoluble particulate material formed in the solution. A further increase of the TAG concentration caused a decrease in turbidity which might be due to the decrease of size or volume fraction of particles. An excess of TAG in mixed solution causes the increase of negative charges, inducing a larger electrostatic and steric repulsion with the decrease of aggregation and formation of smaller particles.

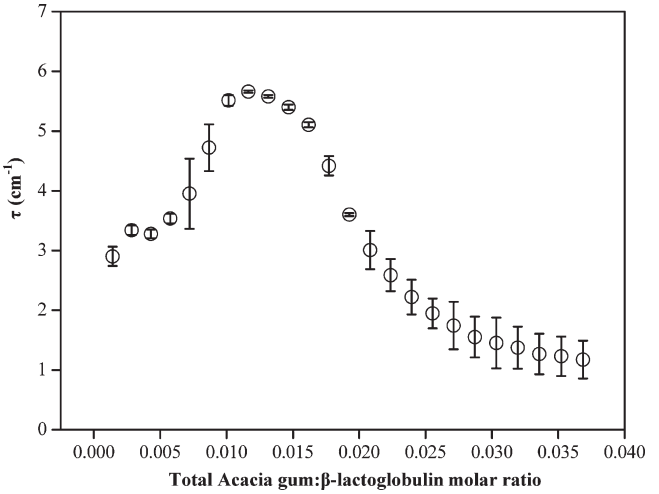

Figure 7. Evolution of turbidity (τ) as a fonction of TAG/BLG molar ratio during the titration of an aqueous dispersion of TAG (1.8 wt %) into an aqueous dispersion of BLG (0.6 wt %) at pH 4.2 and 25 °C. The experiments were made in triplicate.

Optical microscopy was used in parallel to follow the TAG/BLG molar ratio-induced microstructural changes. To observe the structure and size of particle, a concentrated medium (1.5% BLG and 4.5% TAG) was used to better understand the complexation mechanism. Micrographs were taken at different TAG/BLG molar ratio values during titration of BLG dispersion by TAG dispersion at pH 4.2 and 25 °C (Figure 8). A first look on

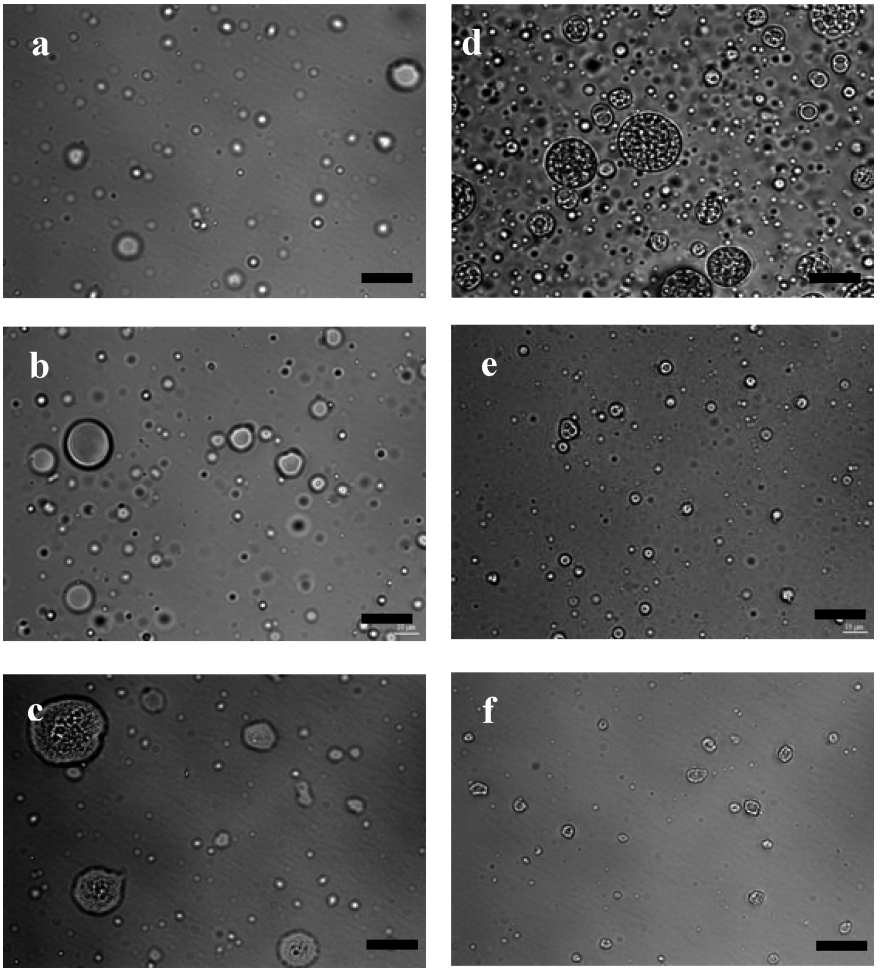

Figure 8. Epi-fluorescence micrographs taken during the titration of an aqueous dispersion of TAG (4.5 wt %) into an aqueous dispersion of BLG (1.5 wt %) at pH 4.2, 25 °C, and different TAG/BLG molar ratio: (a) 0.001; (b) 0.004; (c) 0.008; (d) 0.015; (e) 0.027; (f) 0.033. Bar represents 20 μm. Contrast and brightness of micrograph were treated by the ImageJ freeware (version 1.40).

micrographs reveals that microstructures of dispersions were different, and an effect of the TAG/BLG molar ratio was observed. At a low molar ratio (Figure 8a−c), a great number of coacervates induced by phase separation were visible with apparent diameters (d_a) ranging approximatively from 1 to 10 μm. However, the remarkable feature of the micrograph (Figure 8c) was the appearance of large coalescing coacervates ($d_a \sim 10-25$ μm). The increase of molar ratio of the mixture was characterized by an increase of polydispersity and heterogeneity of the medium. The number of vesicular coacervates considerably increased, and largely more numerous coacervates appeared at a molar ratio of 0.015 (Figure 8d). A number of vesicular coacervates were coalesced or partially coalesced, promoting the formation of multivesicular structures. Two different kinds of morphologies were noticed for the large coacervates. One morphology consisted of a large central vacuole ($d_a \sim 1-4$ μm) surrounded by the coacervated phase which contained smaller vacuoles. The other type of morphology was a homogeneous assembly of vacuoles. At the end of the titration experiment, the major structural characteristic of system was the dominant presence of small coacervates ($d_a \sim 1-5$ μm) and the almost complete disappearance of large vesicles (Figure 8e,f).

Discussion

The occurrence of an exothermic−endothermic sequence upon interactions between a protein and a polysaccharide[37−40] has been reported previously. These complex patterns are very difficult to interpret but seems to be promoted by an increased strength of interactions between biopolymers upon titration, as shown by Langevin dynamics simulation.[56] This assumption is supported by experiments that showed that the endothermic signal is induced, at least partly, directly or indirectly, by aggregation or coacervation of complexes.[37−39]

Coacervation is a phenomenon widely spread in the formation of protein−polysaccharide complexes.[5] Attractive electrostatic interactions between the two biopolymers prevail during complex coacervation, a process which is favored by a low temperature and random coil configurations of both biopolymers.[5] In the case of complex coacervation occurring between weakly charged polyelectrolytes, Ou and Muthukumar[56] recently highlighted the fact that complexation was driven by a negative enthalpy due to electrostatic attraction between two oppositely charged chains, with counterion release entropy playing only a minor role.

The presence of two distinct structuring stages during interaction between TAG and BLG were indicated by calorimetric experiments. The existence of the two-step process involved in this complexation process is in agreement with the Tainaka theory,[57]

(56) Ou, Z.; Muthukumar, M. Entropy and enthalpy of polyelectrolyte complexation: Langevin dynamics simulations. *J. Chem. Phys.* **2006**, *124*, (15), 154902.
(57) Tainaka, K. I. Study of complex coacervation in low concentration by virial expansion method. I. Salt free systems. *J. Phys. Soc. Jpn.* **1979**, *46*, 1899−1906.

which is adapted from the Veis−Aranyi theory[58] based on the complex coacervation between oppositely charged gelatins. In this model, complex coacervation is considered as a two-step process rather than a spontaneous one. Considering the number of BLG dimers interacting with TAG (90 and 80 dimers for the first and the second structuring stage, respectively), Schmitt et al.[40] calculated that there are 86 binding sites per acacia gum molecule. Considering the number of binding sites on a monomeric equivalent of BLG, one found, however, a discrepancy between the calculated sites and the 30 monomers that are able to bind taking into account the biopolymer weight ratio (BLG/TAG = 2:1) at complete saturation.[40,43] Schmitt et al.[40] reported that the likely explanation could be first that BLG does not bind as a monomer but as a dimer (or an equilibrium between monomer−dimer). However, this assumption still does not allow a good fit between the calculated value and the experimental one (58 vs 86). Thus, one may infer that monomeric and/or dimeric BLG are able to saturate more than one theoretical site on the Acacia gum chain, namely, from 1.5 to 3. This multiple-sites binding might be explained by the present of charge patches on the surface of the BLG inducing conformational changes of the polysaccharide backbone and reducing the theoretical number of BLG monomers able to bind.[8,9,59]

The first structuring stage was obviously enthalpically driven at 25 °C due to the major contribution of the exothermic stage, principally induced by electrostatic interaction between BLG and TAG taking place after mixing. Some works suggested that many types of interaction such as hydrogen bonding and van der Waals interactions could be associated with the negative values of ΔH_m and ΔS_m.[60,61] On this basis, it was suggested that the exothermic step in the binding curve contains, in addition to the electrostatic interactions, the contribution of hydrogen bonding. The temperature also had an influence on TAG/BLG interactions by changing the Flory−Huggins interaction energy. Low temperatures are conducive to hydrogen-bond formation, whereas hydrophobic interactions and covalent bonding are enhanced by increasing the temperature, because of the exposure of reactive sites by thermal denaturation of globular proteins and conformational changes of polysaccharide structure.[62] Thus, the decrease of strength of interaction and the disappearance of endothermic peaks with increasing temperature could be attributed to hydrogen-bond breakage. The variation of stoichiometry (N) with temperature could be attributed to the equilibrium displacement toward the monomeric form of BLG[63] or pH variation of the heated TAG. Complexation with lower stoichiometry is in agreement with the formation of protein aggregates during heating, which favors complexation.[32,64] The electrophoretic mobility of TAG was negative at the considered pH in the present study due to the presence of glucuronic acid residues in the gum ($pK_a < 3.6$). The total charges of AG could decrease with decreasing pH because less acidic carboxylic groups became ionized. The pH of the heated TAG dispersion was measured. It slightly decreased from 4.2 (at 25 °C) to 4.15 (at 50 °C). These results indicated that there were no significant changes in pH value with increasing temperature.

Molar heat capacity, ΔC_p, calculated from the slope of the ΔH versus temperature relationship, originated from changes in the degree of surface hydration in free and complexed molecules and to a lesser extent from changes in molecular vibrations.[27] The ΔC_p corresponding to the first stage of interaction was large and positive, a typical signature of ionization/charge neutralization reactions,[37,38,42,65,66] and confirmed a reduction in the number of polar surface-exposed residues.[67] In some cases electrostatic binding between macromolecules was impossible unless strong hydrophobic interactions are generated by heating.[68]

Various studies have been conducted on the effect of temperature on the formation of protein−polysaccharide complexes. The influence of temperature on the kinetics of complex coacervation, was studied by Sanchez et al.[69] on mixed BLG/TAG (pH 3.6, 1:1 BLG/TAG weight ratio and 2% total concentration) at 25 and 50 °C. It was shown that the phase separation appeared faster at 50 °C and the sizes of coacervates were somewhat different at two temperatures. The influence of temperature could be explained by the presence of protein aggregates in BLG dispersion of which may be more responsive to high temperature and accelerate the phase separation. Harding et al.[70] highlighted the effect of temperature on the conformational changes in BSA and the resulting formation of complexes with alginate. Thus, between 35 and 70 °C no complexes were formed, whereas complexes appeared above 70 °C. Complex formation was mainly related to the conformational changes of BSA around its denaturation temperature of 55 °C, so that additional hydrophobic groups could be exposed, favoring complex formation. Similar effects of temperature have been reported upon complex building between gelatin and κ-carrageenan.[71]

The size measurements of formed TAG/BLG complexes indicated major structuring events in the early stage of titration. D_h considerably increased, and turbidity evolution remains constant. It may indicate that certain objects disappear and others appear upon complexation. From this stage, D_h attained its minimum value (∼250 nm), τ displayed a very important acceleration, and particle polydispersity increased with the appearance of second population of particles. These results suggest an increase in the amount of insoluble particulate material formed in the solution.

(58) Veis, A.; Aranyi, C. Phase separation in polyelectrolyte systems. I. Complex coacervates of gelatin. *J. Phys. Chem.* **1960**, *64*, (9), 1203−1210.
(59) Kinsella, J. E. Milk proteins: physicochemical and functional properties. *Crit. Rev. Food Sci. Nutr.* **1984**, *21*, (3), 197−262.
(60) Sakka, K.; Nakanishi, M.; Sogabe, M.; Arai, T.; Ohara, H.; Tanaka, A.; Kimura, T.; Ohmiya, K. Isothermal titration calorimetric studies on the binding of a family 6 carbohydrate-binding module of Clostridium thermocellum XynA with xylooligosaccharides. *Biosci., Biotechnol., Biochem.* **2003**, *67*, (2), 406−409.
(61) Barratt, E.; Bingham, R. J.; Warner, D. J.; Laughton, C. A.; Phillips, S. E. V.; Homans, S. W. Van der Waals interactions dominate ligand-protein association in a protein binding site occluded from solvent water. *J. Am. Chem. Soc.* **2005**, *127*, (33), 11827−11834.
(62) Kelly, R.; Gudo, E. S.; Mitchell, J. R.; Harding, S. E. Some observations on the nature of heated mixtures of bovine serum albumin with an alginate and a pectin. *Carbohydr. Polym.* **1994**, *23*, (2), 115−120.
(63) Aymard, P.; Durand, D.; Nicolai, T. The effect of temperature and ionic strength on the dimerisation of β-lactoglobulin. *Int. J. Biol. Macromol.* **1996**, *19*, (3), 213−221.
(64) Thongngam, M.; McClements, D. J. Characterization of Interactions between Chitosan and an Anionic Surfactant. *J. Agric. Food Chem.* **2004**, *52*, (4), 987−991.
(65) Gomez, J.; Hilser, V. J.; Xie, D.; Freire, E. The heat capacity of proteins. *Proteins* **1995**, *22*, (4), 404−412.
(66) Klocek, G.; Seelig, J. Melittin interaction with sulfated cell surface sugars. *Biochemistry* **2008**, *47*, (9), 2841−2849.
(67) Hileman, R. E.; Jennings, R. N.; Linhardt, R. J. Thermodynamic analysis of the heparin interaction with a basic cyclic peptide using isothermal titration calorimetry. *Biochemistry* **1998**, *37*, (43), 15231−15237.
(68) Zhang, L.; Kosaraju, S. L. Biopolymeric delivery system for controlled release of polyphenolic antioxidants. *Eur. Polym. J.* **2007**, *43*, (7), 2956−2966.
(69) Sanchez, C.; Despond, S.; Schmitt, C.; Hardy, J. Effect of heat and shear on β-lactoglobulin-acacia gum complex coacervation. In *Food Colloids: Fundamentals of Formulation*; Dickinson, E., Miller, R., Eds.; Royal Society of Chemistry: Cambridge, 2001; pp 332−341.
(70) Harding, S.; Jumel, K.; Kelly, R.; Gudo, E.; Horton, J. C.; Mitchell, J. R. The structure and the nature of protein-polysaccharide complexes. In *Food proteins, structure and functionality*; Mothes, K. D. S. a. R., Ed.; VCH: Weinheim, 1993; pp 216−226.
(71) Fang, Y.; Li, L.; Inoue, C.; Lundin, L.; Appelqvist, I. Associative and segregative phase separations of gelatin/κ-carrageenan aqueous mixtures. *Langmuir* **2006**, *22*, (23), 9532−9537.

The total net charge in the TAG/BLG mixed dispersion was negative, and an increase of these negative charges was observed. The most likely explanation concerns the dissociation of TAG aggregates leading to the unmasking of buried negatively charged groups. Mekhloufi et al.[43] indicated that the gain of negative charges in the TAG/BLG mixed dispersion was due entirely to chemical or structural changes affecting TAG. Interactions between oppositely charged biopolymers, as a consequence of strong attractive interactions, usually lead to phase separation and formation of neutral aggregate complexes. Nevertheless, Xia et al.[72] found that the requirement of neutrality at phase separation was not a general rule and was only observed for complexes formed by protein−polycationic polymers. For protein−polyanionic polymers, phase separation occurred for complexes with a negative total charge. No explanation was provided. Similar results were observed by Mekhloufi et al.[43] It is important to note that electrophoretic mobility data reflect only the surface properties of shallow part in fixed charge layer. Some authors[14] indicated that Arabic gum was randomly coil shaped at pH 4.2 and was considered with an ion-penetrable layer at the outer surface exposed to the continuous medium characteristic of soft particles.[73,74] The BLG is a compact globular protein with a hydrodynamic diameter around 4.8 nm and an absolute value of electrophoretic mobility lower than TAG. This finding could be related to the lower charge of BLG. In this situation, the protein needs to be inserted in the deeper layer of the polysaccharide structure to get a strong interaction as the BLG charges are lower, favoring the overlapping in the TAG structure. This finding could help to clarify why the electrophoretic mobility of the TAG/BLG complexes does not converge to zero.

The changes in enthalpy at the second endothermic stage of curves might be due to changes in intermolecular forces of interactions, the presence of a network of interpolymeric complexes, changes in conformation, and the aggregation of biopolymer.[36,44,75−79] Furthermore, it may be expected that the condensation of aggregates arose at this stage, in parallel with the liberation of water molecules from particles. This might produce hydrogen-bonding breakage and lead to the appearance of endothermic peaks. According to the Tainaka theory, the process called complexation begins at this structuring stage, where intrapolymer complexes aggregate to form interpolymer complexes. These aggregates rearrange slowly to form the coacervate phase. The mechanism is driven by an increase of configurational entropy through the formation of a randomly mixed concentrated coacervate phase and dilution of aggregate phase.[58]

Negative ΔC_p observed at this structuring stage is indicative of a hydrophobic contribution to the binding process[65,66] with a change in the solvent-accessible surface area upon binding.[80,81] According to the hydrophobic effect, a negative ΔC_p arises from the release of hydration water if nonpolar, solvent-accessible surface areas meet to form a purely hydrophobic complex.[82]

It is important to note that a consequence of biopolymer complexation was the progressive homogenization of particle sizes in the mixed dispersion. Indeed, D_h of complexes remained steady (300−340 nm) until the end of the titration experiment, and the second population of particles disappeared. These results explain the decrease in turbidity at this structuring stage.

Another surprising feature of the thermodynamics of interaction of TAG with BLG is the presence of entropy−enthalpy compensation (Figure 4) which accompanies the formation of hydrogen bonds.[67,81] Liu et al. (2001)[83] reported the monotonic relationship between the slopes and the correlation coefficients of the $T\Delta S_m - \Delta H_m$ plots of different host−guest systems and indicated that solvent reorganization was the physical origin of the above observed compensation effects.

A large ΔC_p, either negative or positive, leads to significant temperature variations in ΔH_m and ΔS_m which, nevertheless, tend to compensate to give relatively smaller changes in the more functionally significant ΔG_m (Tables 1 and 2), which is then less sensitive to temperature fluctuation.[81]

Conclusion

Thermodynamic characterization of TAG/BLG interactions was studied using ITC in aqueous dispersion of pH 4.2 combining with DLS, electrophoretic mobility, turbidity measurements, and optical microscopy as complementary methods on titration mode.

Calorimetric experiments indicate the presence of two distinct structuring stages during interaction between TAG and BLG. The first step is obviously enthalpically driven with unfavorable binding entropy, principally because of the direct electrostatic interaction between the BLG and the TAG. The positive ΔC_p at this step is the signature of electrostatic interactions and due to reduction in the number of polar surface-exposed residues. This exothermic step in the binding curve contains, in addition to the electrostatic interactions, the contribution of hydrogen bonding. During the second binding step, the reaction becomes entropy-driven. Intrapolymer complexes aggregate and condense to form dense supramolecular structures. Change in the solvent-accessible surface area upon binding is the primary contributor to negative ΔC_p value, which is indicative of hydrophobic contributions to the binding process.

The observed exothermic−endothermic sequence suggested other energetic contributions such as the liberation of water molecules and ions, conformational changes of biopolymers, and/or the aggregation of protein−polysaccharide complexes.

(72) Xia, J.; Dubin, P. L.; Kokufuta, E. Dynamic and electrophoretic light scattering of a water-soluble complex formed between pepsin and poly(ethylene glycol). *Macromolecules* **1993**, *26*, (24), 6688−6690.
(73) Ducel, V.; Saulnier, P.; Richard, J.; Boury, F. Plant protein-polysaccharide interactions in solutions: application of soft particle analysis and light scattering measurements. *Colloids Surf., B* **2005**, *41*, (2−3), 95−102.
(74) Tsuneda, S.; Aikawa, H.; Hayashi, H.; Hirata, A. Significance of cell electrokinetic properties determined by soft-particle analysis in bacterial adhesion onto a solid surface. *J. Colloid Interface Sci.* **2004**, *279*, (2), 410−417.
(75) Lu, C.; Pelton, R.; Valliant, J.; Bothwell, S.; Stephenson, K. Colloidal flocculation with poly(ethylene oxide)/polypeptide complexes. *Langmuir* **2002**, *18*, (11), 4536−4538.
(76) Rutten, A. A. C. M.; Bouwman, W. G.; van der Leeden, M. C. β-Lactoglobulin as an ideal random polymer coil. *Colloids Surf., A* **2002**, *210*, (2−3), 243−252.
(77) Bai, G.; Nichifor, M.; Lopes, A.; Bastos, M. Thermodynamic characterization of the interaction behavior of a hydrophobically modified polyelectrolyte and oppositely charged surfactants in aqueous solution: Effect of surfactant alkyl chain length. *J. Phys. Chem. B* **2005**, *109*, (1), 518−525.
(78) Csaki, K. F.; Nagy, M.; Csempesz, F. Influence of the chain composition on the thermodynamic properties of binary and ternary polymer solutions. *Langmuir* **2005**, *21*, (2), 761−766.
(79) Bordbar, A.-K.; Taheri-Kafrani, A.; Mousavi, S. H.-A.; Haertlé, T. Energetics of the interactions of human serum albumin with cationic surfactant. *Arch. Biochem. Biophys.* **2008**, *470*, (2), 103−110.
(80) Baker, B. M.; Murphy, K. P. Prediction of binding energetics from structure using empirical parameterization. *Methods Enzymol.* **1998**, *295*, 294−315.
(81) Cooper, A. Heat capacity of hydrogen-bonded networks: an alternative view of protein folding thermodynamics. *Biophys. Chem.* **2000**, *85*, (1), 25−39.
(82) Brockhaus, M.; Ganz, P.; Huber, W.; Bohrmann, B.; Loetscher, H. R.; Seelig, J. Thermodynamic studies on the interaction of antibodies with β-amyloid peptide. *J. Phys. Chem. B* **2007**, *111*, (5), 1238−1243.
(83) Liu, L.; Yang, C.; Mu, T. W.; Guo, Q. X. A Statistical Examination on the Compensation between the Enthalpies and Entropies Obtained from the Calorimetric Methods. *Chin. Chem. Lett.* **2001**, *12*, (2), 167−170.

The results obtained by the complementary methods shows that the binding process is affected by the TAG/BLG molar ratio. The hydrodynamic diameter, electrophoretic mobility, and turbidity of TAG/BLG mixed dispersion increased with the molar ratio. These results suggest an increase in the amount of insoluble particulate material formed in the solution. The different parameters reach maximum values at the TAG/BLG molar ratio corresponding to the saturation ratio of binding determined from ITC binding curves, where the release binding was reversed to endothermic. It would correspond to a maximum number of particles present in dispersions, in agreement with a maximum strength of interaction. D_h attained its minimum value; τ displayed a very important acceleration, and particle polydispersity increased with the appearance of a second population of particles. This could reveal the instability of the system caused by aggregation or coalescence of particles.

A further increase of the TAG concentration caused a decrease in turbidity which might be due to the decrease of size or volume fraction of particles. The mixed μ_E displayed a similar whole evolution than TAG alone, indicating a good accessibility of the polysaccharide to the solvent. This highlighted the main contribution of TAG to the μ_E evolution of a mixed dispersion. The present study tried to better understand thermodynamic mechanisms at the origin of binding processes and stabilization of TAG/BLG assemblies, the use of complementary methods would be useful to understand the nature of interactions involved between TAG and BLG and the extent of complex formation.